ACS OMEGA

Open Access

http://pubs.acs.org/journal/acsodf

Article

Mitigating Acetaminophen-Induced Kidney Injury: The Protective Role of Grape Seed and Peanut Skin Extracts through the iNOS/CYP2E1 Pathway

Samah A. El-Hashash, Wafaa A. Gaballah, Asmaa Antar Faramawy, Nermin I. Rizk, Meshari A. Alsuwat, Mohammed Ali Alshehri, Samy M. Sayed,* and Mustafa Shukry*

Cite This: *ACS Omega* 2024, 9, 35154−35169

Read Online

ACCESS | Metrics & More | Article Recommendations | Supporting Information

ABSTRACT: The rising number of acute kidney injury cases worldwide due to acetaminophen (APAP) emphasizes the critical need for effective prevention strategies to counteract APAP's detrimental effects. This study examined the kidney-protective capabilities of ethanolic extracts from grape seeds and peanut skins (GSEE and PSEE, respectively) in comparison with silymarin in rats that experienced an APAP overdose. The phenolic compounds in these extracts were measured by using high-performance liquid chromatography (HPLC). In the experiment, Sixty adult male albino rats were divided into five groups of 12. The Control group received 0.5 mL of saline via a gastric tube. Group II received acetaminophen (APAP, 640 mg/kg per day via a gastric tube) to induce renal injury, following Ucar et al. and Islam et al. Groups III, IV, and V received silymarin (50 mg/kg), grape seed extract (200 mg/kg), and peanut skin extract (200 mg/kg), respectively, along with 640 mg of APAP/kg per day for 21 days. Post APAP treatment, significant increases in serum urea and creatinine levels were noted, along with notable decreases in the percentage of body weight gain. Furthermore, there were increases in oxidative stress and inflammatory markers in the kidney tissues, including heightened mRNA expressions of renal iNOS and CYP2E1, which were confirmed through histological studies. The administration of GSEE, PSEE, and silymarin mitigated these adverse effects, likely due to their high phenolic content, which is recognized for its antioxidant and anti-inflammatory effects. GSEE, in particular, showed efficacy comparable to that of silymarin. Molecular docking studies revealed that APAP impeded critical enzymes essential for cellular antioxidant defense, whereas the bioactive compounds in the grape seed and peanut skin extracts effectively inhibited key enzymes and receptors involved in inflammation and oxidative stress. These findings suggest that GSEE and PSEE could serve as viable alternative treatments for kidney damage induced by APAP. Further research to isolate and identify these effective compounds is recommended.

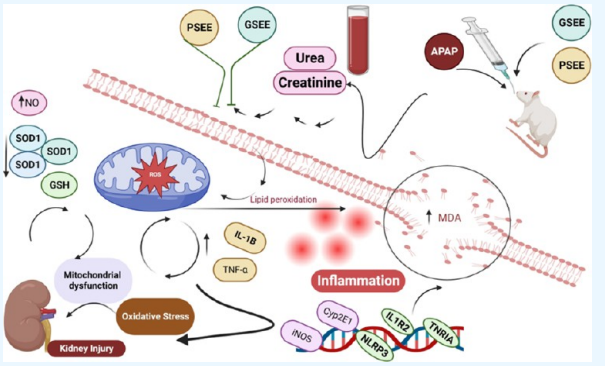

1. INTRODUCTION

There is a high prevalence of acute kidney injury (AKI) across all clinical departments with an independent relation to high morbidity and mortality rates. One of the most important reasons for AKI is nonsteroidal anti-inflammatory drugs (NSAIDs). Paracetamol, whose chemical name is acetaminophen (APAP), is the most well-known pain reliever and antipyretic among these drugs.[1] Numerous interrelated factors were reported to contribute to APAP-induced nephrotoxicity, resulting in kidney damage. They include reactive oxygen species (ROS) generation, inflammatory response promotion, and hemodynamic abnormal changes.[2] Between 2 and 10% of individuals who have an overdose of APAP will get acute renal impairment, whether or not hepatotoxicity is present.[3] One byproduct of acetaminophen (APAP) breakdown by cytochrome P450 enzymes in the kidney is the poisonous metabolite *N*-acetyl-*P*-benzoquinone-imine. This metabolite contributes to the renal tubular dysfunction observed in APAP-induced kidney injury. *N*-Deacetylase enzymes and prostaglandin synthetase have also been implicated in this process.[4]

APAP-induced toxicity has increased in the developing world over the past few years. In Egypt, hospital-based prospective studies, from 2015 via the COVID-19 pandemic and until now, reported high percentages of APAP-intoxicated cases.[5] Over-the-counter (OTC) and prescription formulations are available, and they can be found in single- and multicomponent forms.[6] Despite its many therapeutic advantages, the unmonitored utilization of APAP is a

Received: June 13, 2024
Revised: July 22, 2024
Accepted: July 23, 2024
Published: July 30, 2024

concerning issue that needs attention to avoid the high incidence of accidental toxicity. Preventing oxidative injury and reducing the inflammatory response is crucial in safeguarding the kidney from APAP toxicity.[7]

In the previous several decades, there has been considerable emphasis on finding new therapeutic strategies, particularly of natural origin, for modulating oxidative stress and inflammation-induced health disorders.[8] This is because allopathic medicines, rather than their high cost, usually have side consequences and alter the properties of life. Consequently, herb extracts and their bioactive compounds may be suitable and safer alternatives.

The dried seeds and fruits of the milk thistle plant are the source of silymarin (Silybum marianum), which has been extensively utilized as a health booster because of its chemical components, such as polyphenols, flavonolignans, and flavonoids. Its antioxidant and anti-inflammatory characteristics have been well documented.[9] Modern evidence suggests that silymarin may promote kidney health and has renoprotective properties.[10] Grape (*Vitis vinifera* L.) seeds are a significant food residue known for their abundant nutrients and substantial medicinal worth. Grape seed extract predominantly comprises 15 phenolic compounds, including (−)-epicatechin, (+)-catechin, gallate, proanthocyanidin, and flavonols. Multiple reports have confirmed GSE's antioxidant, anti-inflammatory, and other beneficial consequences.[11] Moreover, it was reported to maintain kidney function and structure, and its renoprotective effects were cited in many animal studies.[12]

Peanut (*Arachis hypogea* L) skins, considered low-value byproducts in the peanut industry, are rich in polyphenols and fiber. Their color ranges from light brown to deep red. Studies have shown a significant correlation between peanut skins' redness, hue angle, and total polyphenol content. Furthermore, these color attributes strongly correlate with antioxidant capacity, reinforcing the link between total polyphenols and antioxidant effectiveness.[13] As a source of many bioactive ingredients, the renoprotective effects of peanut skin extracts (PSE) were supported by many studies.[14] Several compounds were identified in grape seed ethanolic extract (GSEE) and peanut skin ethanolic extract (PSEE) with notable physiological activities. Gallic acid, with antioxidant, anti-inflammatory, and anticarcinogenic properties, was present at 0.473% in GSEE and 0.019% in PSEE.[15] Protocatechuic acid, known for its antioxidant, antibacterial, and antidiabetic effects, was found at 0.166% in GSEE and 0.481% in PSEE.[16] *p*-Hydroxybenzoic acid, offering antioxidant, anti-inflammatory, cardioprotective, and neuroprotective benefits, was present at 0.059% in GSEE and 0.017% in PSEE.[17] Gentisic acid, with antioxidant, anti-inflammatory, and renal protective effects, was detected only in PSEE at 0.008%.[18] Catechin, known for its anti-inflammatory, antioxidant, and cardiovascular protective properties, was found at 0.5275% in GSEE and 0.0517% in PSEE.[19] Chlorogenic acid, associated with weight loss, antidiabetic, and liver health benefits, was present at 0.00136% in GSEE and 0.00176% in PSEE.[20] Caffeic acid, which has antioxidant, anticancer, and anti-inflammatory effects, was found at 0.00085% in GSEE and 0.00548% in PSEE.[21] Syringic acid, offering antioxidant, antimicrobial, and antidiabetic properties, was not detected in either extract.[22] Vanillic acid, known for its antioxidant, hepatoprotective, and anti-inflammatory benefits, was found at 0.00020% in GSEE and 0.00084% in PSEE.[23] Ferulic acid, which has antioxidant, antiaging, and sun damage protection properties, was present at 0.00295% in GSEE and 0.00394% in PSEE.[24] Sinapic acid, offering antioxidant, anti-inflammatory, and antimicrobial activities, was found at 0.039% in GSEE and 0.018% in PSEE.[25] Rutin, known for its blood vessel protection and anti-inflammatory effects, was present at 0.00823% in GSEE but not detected in PSEE.[26] *p*-Coumaric acid, associated with antioxidant, antidiabetic, and cholesterol-lowering benefits, was not detected in GSEE but found at 0.0332% in PSEE.[27] Apigenin-7-glucoside, with antioxidant, anti-inflammatory, anxiolytic, antidepressant, and antidiabetic effects, was present at 0.054% in GSEE and 0.057% in PSEE.[28] Rosmarinic acid, offering antioxidant, anti-inflammatory, and antiallergic properties, was found at 0.036% in GSEE and 0.041% in PSEE.[29] Cinnamic acid, known for its antioxidant, anti-inflammatory, and antidiabetic effects, was present at 0.002% in GSEE and 0.023% in PSEE.[30] Quercetin, with antioxidant, antihistamine, and anti-inflammatory benefits, was found at 0.086% in GSEE and 0.026% in PSEE.[31] Chrysin, known for its antioxidant, anti-inflammatory, antidiabetic, sleep quality improvement, and antiaromatase activity, was present at 0.001% in GSEE and 0.010% in PSEE.[32] This study compared the renoprotective effects of grape seeds and peanut skins' ethanolic extracts vs silymarin (a valuable component in therapeutic interventions for liver health and beyond[33]) in paracetamol-overdosed rats.

2. MATERIAL AND METHODS

2.1. Plant Materials. At the local market in Gharbia, Egypt, we purchased grapefruits (*V. vinifera* L., variety RoumyAhmer) and peanut pods (*A. hypogea* L.). After authentication by a senior botanist, grapefruits were cleaned and free from the evidence of insect infestation and objectionable materials. Seeds were detached from the pulp and dried in the shade. Regarding peanut pods, they were mildly roasted and manually shelled, and then the skins were removed. After that, both materials were ground using a grinder and frozen at −20 °C until extraction. To prepare ethanolic extracts, 2 kg of each powder was blended with 4 L of ethanol (95%) at ambient temperature. This was done for 3 days with a stirrer in total darkness. The blends were filtered and immersed in a rotating evaporator to remove solvent at 40 ± 5 °C. Yield was 33.9% and 32.45% of grape seed ethanolic extract (GSEE) and peanut skin ethanolic extract (PSEE), respectively.

2.2. Drugs, Chemicals, and Reagents. Acetaminophen (*N*-acetyl-*p*-aminophenol, APAP). Impurities: trace amounts of 4-aminophenol, less than 0.01%, and saline (0.9%) were purchased from Pharma Trade Co., Mansoura, Dakahlia Governorate, Egypt. Silymarin was obtained from SEDICO. Pharmaceutical Co. Giza, Egypt, in the form of sachets, each containing 140 mg. Impurities: less than 0.5% of silibinin, less than 0.1% of isosilybin ethanol (95%), formalin. Al-Gomhoria Co. of Cairo, Egypt, supplied the chemicals and other materials. Sigma, located in St. Louis, MO, provided the diagnostic kits.

2.3. Phenolic Compounds Specification. The method employed to analyze the phenolic profiles of grape seeds and peanut skins involved a detailed process. Initially, the samples were transferred to quick-fit conical flasks with 20 mL of 2 M sodium hydroxide. These flasks were then flushed with N2 gas and securely sealed. The mixtures were agitated for 4 h at ambient temperature, after which the pH was neutralized to 2 using hydrochloric acid (6M). Following centrifugation at

https://doi.org/10.1021/acsomega.4c05534
ACS Omega 2024, 9, 35154−35169

5000 rpm for 10 min, the supernatant was separated for further analysis. Phenolic compounds were then extracted in two stages using a 50 mL mixture of ethyl ether and ethyl acetate in equal proportions. After the organic phase was separated, the solvents were evaporated off at 45 °C; then, the remaining residues were dissolved in 2 mL of methanol for subsequent high-performance liquid chromatography (HPLC) analysis.

We followed the protocol for HPLC analysis laid out by Kim et al.[34] using an Agilent Technologies 1100 series LC system with an autosampler and diode-array detector, utilizing an Eclipse XDB-C18 column and a C18 guard column from Phenomenex. The mobile phase included acetonitrile and acetic acid (2%) in water, with a flow rate of 0.8 mL/min over 60 min. The gradient shifted from 100% solvent B to 0% B, utilizing a 50 μL injection volume. Detection was performed at 280, 320 nm (for benzoic and cinnamic acids), and 360 nm (for flavonoids). Samples were prefiltered through a 0.45 μm filter. Peaks were identified by matching retention times and UV spectra to known standards.

2.4. Animals. The Animal Ethics Committee of the Faculty of Veterinary Medicine approved the animal experiments at the University of Kafrelsheikh (KFS-IACUC/133/2023), adhering to the National Committee for Research's animal care guidelines and scientific use guidelines.

Sixty adult male Sprague-Dawley rats, with 150−160 g of body weight, were procured from the Helwan Farm, VI Org., Cairo, Egypt. They were accommodated in polypropylene cages within a laboratory setting regulated for temperature at 22 ± 1 °C, humidity at 50 ± 20%, and a 12 h cycle of light and darkness. Unlimited access to water was provided, along with a week for acclimatization to the lab conditions before the experiment's commencement. Their diet, supplied by the Company of Agricultural Development in 6-October, Giza, Egypt, was a balanced mix containing 15% sunflower oil and a 45% concentrate mixture. This mixture comprised 49% yellow corn, 11% soybean meal, 10% wheat bran, 3% molasses, 0.7% DL-methionine, 0.5% common salt, 0.2% lysine, 0.2% ground limestone, and 0.1% dicalcium phosphate and included a mineral−vitamin premix.

2.5. Study Design and Sampling. The rats were weighed and then randomly separated into 5 groups, each comprising 12 rats. The first group (Control group) was given normal saline at 0.5 mL/rat through a gastric tube. Group II got acetaminophen (APAP, 640 mg/kg body weight/day using gastric tube) (+ve control) following Ucar et al. and Islam et al.[35−37] to induce acute renal injury in rats. Groups III−V got silymarin (Madaus, Cologne, Germany) (50 mg/kg, as reference control),[38] 200 mg/kg of grape seed ethanolic extract (GSEE), and 200 mg/kg of peanut skin ethanolic extract (PSEE), respectively, along with 640 mg APAP/kg body weight/day for 21-day using gastric tube. APAP, GSEE, and PSEE were dissolved in freshly prepared distilled water by dissolving silymarin in a distilled water solution with 0.5% sodium carboxymethyl cellulose (CMC-Na). Effective non-toxic doses of GSEE and PSEE were selected according to previous studies on animals.[37,39] The APAP was given concurrently with the other substances.

A 21-day feeding study followed Baskaran et al. and Mokhtari et al.[40] At the same time, water and food were provided ad libitum, and their weight was measured weekly. Extracts were given according to the body weight of the rats.

Following the experiment's end, the rats underwent fasting overnight, were then weighed, and had blood samples collected from the retro-orbital venous plexus. The serum was extracted by centrifuging the collected blood at 3000 rpm for 10 min at ambient temperature. The serum was then transferred to an Eppendorf tube and frozen at −20 °C for subsequent analyses.

After the blood was collected, the rats were sedated with an intraperitoneal injection of pentobarbital sodium (70 mg/kg), ensuring a humane euthanasia process. The kidneys were carefully removed, cleansed with a cold saline solution (0.9%), blotted dry, and weighed. A fragment of the right kidney was preserved at −80 °C for molecular and biochemical analysis. In contrast, a piece of the left kidney was fixed in buffered neutral formalin (10%), preparing it for histopathological examinations.

2.6. Homogenate Preparation of Renal Tissues. To evaluate oxidative load markers, 0.2 g of the right kidney tissue was individually homogenized in 1.8 mL of cold homogenizing buffer (pH 7.2) at 0 °C by using a Teflon pestle homogenizer. Subsequently, the resulting mixture was centrifuged at 3000 rpm for 10 min, and the supernatant was preserved at −20 °C until further use. The frozen right kidney tissue was homogenized for cytokine measurement in 1.5 mL RIPA buffer (pH 7.6) containing protease inhibitors at 4 °C. Following a 30 min incubation on ice, the homogenate was centrifuged at 10,000*g* for 30 min at 4 °C, and the supernatants were kept at −80 °C. For the molecular investigation (mRNA expression of iNOS and CYP2E1), 25−30 mg of the right kidney tissue was homogenized using a sterilized manual mortar. Subsequently, 0.6 mL of lysis buffer along with 2-mercaptoethanol was added. The mixture was vortexed for at least 40 s, followed by adding one volume of 70% ethanol to each cell homogenate and further vertexing to ensure thorough mixing and disperse any visible residues, following the manufacturer's recommendations.

2.7. Body Weight and Kidney Relative Weight. Body weight gain (BWG) was estimated by calculating the difference between each rat's final and initial weights. Additionally, the BWG% was calculated by dividing the BWG by the initial weight of each rat, followed by multiplying that quotient by 100. The relative kidney weight (RKW) was calculated using the method outlined by Angervall and Carlström.[41]

2.8. Biochemical Analysis. The urea and creatinine quantities in the serum were assessed using the methodologies outlined by Patton and Crouch[42] for urea determination and by Houot[43] for creatinine determination. The malondialdehyde (MDA) content, indicative of lipid peroxidation, in the homogenate from the right kidney tissue was investigated using the protocol of Ohkawa et al.[44] The nitric oxide (NO) levels were estimated using the methodology outlined by Miranda et al. in their study.[45] Furthermore, the assessments of superoxide dismutase (SOD) activity and reduced glutathione (GSH) levels were performed following the protocols described,[46] respectively. The quantification of pro-inflammatory cytokines in the right kidney tissue, specifically TNF-α and IL-1β, was conducted using an ELISA Kit supplied by Peprotech, following the preparation guidelines for 96-well plates. The analysis was completed using an ELISA plate reader, measuring absorbance at 405 nm with a correction at 650 nm.[47]

2.9. Quantitative Reverse Transcription Polymerase Chain Reaction (qRT-PCR). RNA purity from right kidney tissue samples was determined using a Bio-Rad spectrophotometer at an optical density (OD) of 260/280 nm. Then, 1 μg of RNA was reverse transcripted into single-stranded complementary DNA (cDNA) using the Quanti-Tect reverse

https://doi.org/10.1021/acsomega.4c05534
ACS Omega 2024, 9, 35154−35169

Table 1. qRT-PCR Primer

gene	primer	sequences (5′→3′)	accession no	amplicon size (bp)
iNOS	forward	5′-GGGCCACCTTTATGTTTGTG-3′	(NM_012611.3)	220
	reverse	5′-CCGGTGGGTTTCTTCTTCTTGAA-3′		
CYP2E1	forward	5′-ACTTCTACCTGCTGAGCAC-3′	(NM_031543.1)	221
	reverse	5′-TTCAGGTCTCATGAACGGG-3′		
GAPDH	forward	5′-ATGGGAGTTGCTGTTGAAGTCA-3′	(NM_017008.4)	164
	reverse	5′-CCGAGGGCCCACTAAAGG-3′		

transcription kit (Qiagen, Hilden, Germany). This cDNA was amplified and quantified through a two-step RT-PCR process utilizing the SYBR Green Master Mix kit within a Bio-Rad thermal cycler. The specific primer sequences used are detailed in Table 1 (Qiagen, Germany). The expression levels of target genes, namely, iNOS and CYP2E1, were analyzed using the $2^{-\Delta\Delta CT}$ method, with GAPDH as the normalization reference gene.

2.10. Kidney Histopathology. The samples of the left kidney were dehydrated in increasing serial ethanol and cleaned with xylene; then, they were left in neutral formalin buffered with 10% phosphate for a full day. The slices were then sectioned at a 5 μm thickness and treated into paraffin blocks. These sections underwent routine histological staining techniques with hematoxylin and eosin (H&E).[48]

2.11. Molecular Docking. The study utilized a Windows 10 Pro system with an Intel(R) Core(TM) i7-5500U CPU and DDR4 RAM, leveraging the AlphaFold database (https://alphafold.ebi.ac.uk/) and MOE 2022.02 software for molecular docking and data retrieval. For the protein and ligand formulation, the three-dimensional (3D) models of APAP, silymarin, and the active ingredients from grape seed and peanut skin extracts were obtained in SDF format from the PubChem database and processed with the MOE software for energy optimization and protein docking.

The 3D configurations of rat proteins, including glutathione synthetase, superoxide dismutase-1 (SOD1), SOD2, SOD3, tumor necrosis factor receptor superfamily member 1A (TNR1A), interleukin-1 receptor type 2 (IL1R2), cytochrome P450 2E1 (Cyp2e1), and inducible nitric oxide synthase (iNOS), were acquired from the AlphaFold protein structure database. These target proteins were prepped for docking in the MOE software by eliminating any water and ligand molecules from their structures and performing energy minimization on the proteins. For investigating and visualizing molecular docking, the ligands were docked to target proteins using MOE software, which involved pinpointing the binding site and employing an induced fit docking model. Subsequently, the protein and ligand interactions were visualized by using the same software.

2.12. Statistical Analysis. Before analyzing the data, the data set was checked for a normal distribution, linear associations, and consistent variance using Kolmogorov-Smirnov and Levene's tests. Data represented as means ± standard errors were used to report anthropometric and biochemical findings. A one-way analysis of variance (ANOVA) was performed, and post hoc descriptive tests (Dunnett's and Duncan's) were used to examine the data, with SPSS version 22 for Windows serving as the main platform (SPSS, IBM, Chicago, IL). A p-value of 0.05 or lower was deemed statistically significant.

3. RESULTS

3.1. Phenolic Profile of GSEE and PSEE. The HPLC analysis identified 15 phenolic compounds in grape seed ethanol extract (GSEE) at detectable levels, as shown in Table 2. They vary significantly in concentration, being the major

Table 2. HPLC Analysis of the Phenolic Profile of Both GSEE and PSEE

compound	GSEE (μg/g)	PSEE (μg/g)
gallic	4733.22	185.45
protocatechuic	165.52	480.59
p-hydroxybenzoic	59.67	16.64
gentisic	ND	7.79
catechin	5274.88	517.39
chlorogenic	13.60	17.56
caffeic	8.49	54.79
syringic	ND	ND
vanillic	2.02	8.41
ferulic	29.50	39.42
sinapic	38.81	17.85
rutin	82.25	ND
p-coumaric	ND	331.51
apigenin-7-glucoside	53.88	56.68
rosmarinic	36.44	40.84
cinnamic	1.61	22.76
qurecetin	8.64	26.36
apigenin	ND	ND
kaempferol	ND	ND
chrysin	0.75	10.25

catechin (5274.88 μg/g). Gallic acid was the second compound found abundantly (4733.22 μg/g). The compounds found in somewhat small concentrations were protocatechuic acid (165.52 μg/g), rutin (82.25 μg/g), p-hydroxybenzoic (59.67 μg/g), and apigenin-7-glucoside (53.88 μg/g). The compounds found in small amounts were sinapic, rosmarinic, and ferulic acids (38.81, 36.44, and 29.50 μg/g, respectively). The other six compounds in minimal concentrations ranged between 0.75 μg/g (chrysin) and 13.60 μg/g (chlorogenic acid). Of them, quercetin was the most important and was found at a concentration of 8.64 μg/g, nearly the same as caffeic acid, which was 8.49 μg/g (Table S1 and Figure S1).

As for PSEE, 16 phenolic compounds were found in the detected levels. Like GSEE, phenolic compounds in PSEE varied in their concentrations; however, their variation was not significant, with the major being catechin (517.39 μg/g), followed by protocatechuic (480.59 μg/g), p-coumaric (331.51 μg/g), and gallic (185.45 μg/g) acids. The compounds found in medium concentrations were apigenin-7-glucoside, caffeic acid, rosmarinic acid, and ferulic acid (56.68, 54.79, 40.84, and 39.42 μg/g, respectively). The other eight compounds were discovered in small quantities ranging between 7.79 μg/g

https://doi.org/10.1021/acsomega.4c05534
ACS Omega 2024, 9, 35154−35169

Table 3. Effects of Grape Seeds and Peanut Skin Ethanolic Extracts vs Silymarin on Body Weight and Kidney Relative Weight in Acetaminophen-Overdosed Rats[a]

parameters	control	APAP	silymarin	GSEE	PSEE	*P*-value
Initial b.w. (g)	156.1 ± 6	152.1 ± 2	158 ± 6	154 ± 6	159.2 ± 7	0.937
Final b.w. (g)	184.2 ± 4	175.4 ± 2	186.6 ± 3	183.3 ± 2	184.6 ± 3	1.000
BWG (g)	28.1 ± 2.0^{a}	23.3 ± 2.0^{b}	28.6 ± 3.1^{a}	29.3 ± 2.1^{a}	25.4 ± 1.6^{b}	0.010
BWG (%)	18.01 ± 1.0^{a}	15.31 ± 2.0^{b}	18.10 ± 2.5^{a}	19.02 ± 2.4^{a}	15.95 ± 1.9^{b}	0.001
AKW (g)	1.1 ± 0.1	1.0 ± 0.1	1.2 ± 0.2	1.1 ± 0.2	1.2 ± 0.1	0.721
RKW (%)	0.60 ± 0.1	0.57 ± 0.1	0.64 ± 0.1	0.60 ± 0.1	0.65 ± 0.1	0.781

[a]Data are reported as means ± SEM. Values bearing unique superscripts ($^{a, b}$) in the same row indicate significant differences, with a significance threshold set at $p < 0.05$. Abbreviations used are APAP for acetaminophen, GSEE for grape seed ethanolic extract, and PSEE for peanut skin ethanolic extract. BWG, body weight gain. AKW, absolute kidney weight; RKW, relative kidney weight.

Table 4. Effect of Grape Seeds and Peanut Skin Ethanolic Extracts vs Silymarin on Kidney Function Markers in Acetaminophen-Overdosed Rats[a]

group parameters	control	APAP	silymarin	GSEE	PSEE	*P*-value
urea (mg/dL)	23.7 ± 2.97^{a}	71.1 ± 8.90^{d}	35.2 ± 4.38^{b}	43.2 ± 5.40^{bc}	49.3 ± 6.16^{c}	0.001
creatinine (mg/dL)	0.560 ± 0.07^{a}	1.140 ± 0.14^{d}	0.690 ± 0.09^{ab}	0.810 ± 0.10^{bc}	0.870 ± 0.11^{c}	0.001

[a]Data are displayed as means ± standard deviations (SD). Different superscript letters (a, b, c) within the same row indicate a significant variance at a *p*-value less than 0.05. APAP represents acetaminophen, GSEE is for grape seed ethanolic extract, and PSEE denotes peanut skin ethanolic extract.

Table 5. Effect of Grape Seeds and Peanut Skin Ethanolic Extracts vs Silymarin on Oxidative/Antioxidant Profile in Kidney Tissue Homogenates of Acetaminophen-Overdosed Rats[a]

group parameters	control	APAP	silymarin	GSEE	PSEE	*P*-value
MDA (nmol/g)	5.15 ± 0.64^{a}	12.97 ± 1.62^{d}	6.81 ± 0.84^{b}	8.13 ± 1.03^{bc}	9.02 ± 1.13^{c}	0.001
NO (μmol/g)	1.66 ± 0.20^{a}	3.90 ± 0.48^{d}	2.21 ± 0.27^{b}	2.66 ± 0.34^{bc}	2.97 ± 0.38^{c}	0.001
GSH (mmol/g)	1.70 ± 0.20^{d}	0.58 ± 0.06^{a}	1.50 ± 0.19^{cd}	1.34 ± 0.17^{bc}	1.17 ± 0.14^{b}	0.001
SOD (U/g)	168 ± 21^{d}	60 ± 8^{a}	124 ± 16^{c}	109 ± 14^{bc}	96 ± 12^{b}	0.001

[a]Data are presented as means ± standard deviations (SD). Values labeled with distinct superscript letters within a single row indicate significant discrepancies at a *p*-value less than 0.05. APAP signifies acetaminophen, GSEE stands for grape seed ethanolic extract, PSEE represents peanut skin ethanolic extract, MDA is malondialdehyde, NO denotes nitric oxide, GSH refers to reduced glutathione, and SOD is superoxide dismutase.

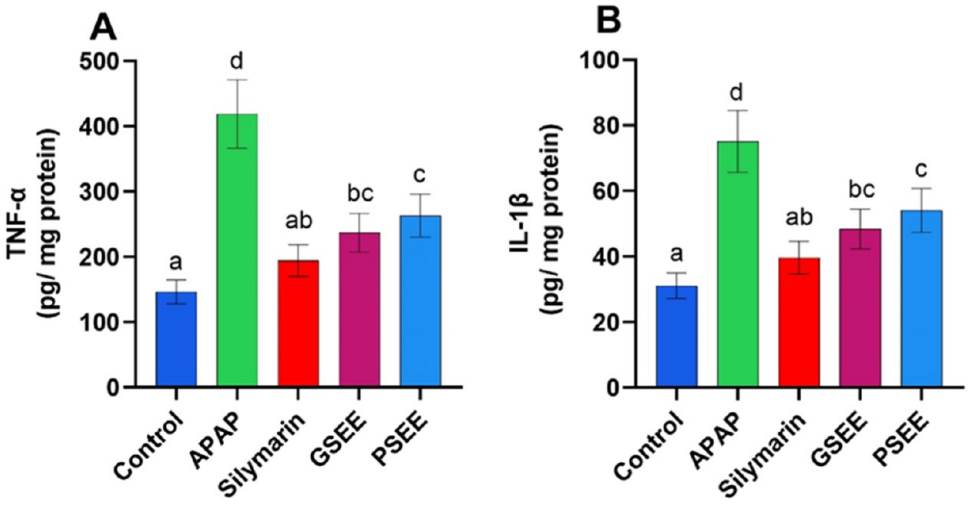

Figure 1. Impact of ethanolic extracts from grape seeds and peanut skins versus silymarin on inflammatory markers in kidney tissue homogenates of rats with an acetaminophen overdose. The findings are reported as means ± standard deviations (SD). In each row, a,b, and c values carrying unique superscript letters denote significant variation at a *p*-value below 0.05. Abbreviations include APAP for acetaminophen, GSEE for grape seed ethanolic extract, PSEE for peanut skin ethanolic extract, TNF-α for tumor necrosis Factor-α, and IL-1β for interleukin-1β.

(gentisic acid) and 26.36 μg/g (quercetin) (Table 2). Of them, chlorogenic and cinnamic acids were found at 17.56 and 22.76 μg/g concentrations, respectively (Table S2 and Figure S2).

3.2. Anthropometric Markers. The rats' body weight was recorded during the pre and postexperiment course. No significant differences ($p > 0.05$) in their final weight rather than initial weight were observed among study groups. In addition, BWG % of APAP-overdosed rats was substantially less than that of the control group ($p < 0.05$). Administration of either silymarin or GSEE along with APAP induced a

https://doi.org/10.1021/acsomega.4c05534
ACS Omega 2024, 9, 35154−35169

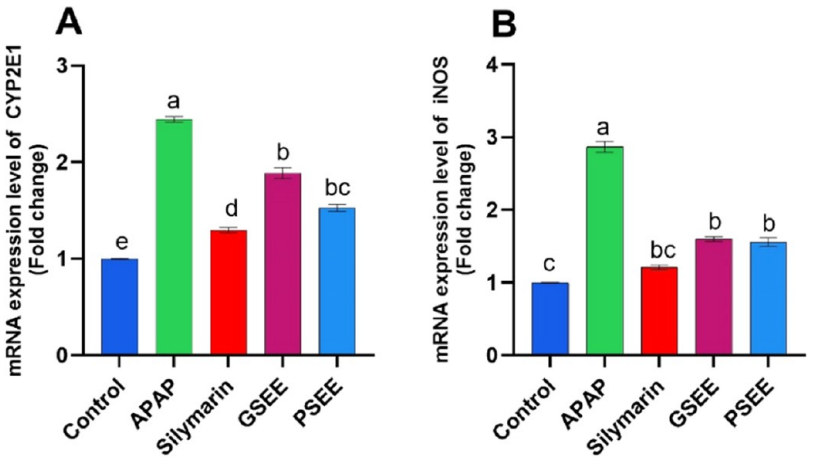

Figure 2. Influence of ethanolic extracts from grape seeds and peanut skins compared to silymarin on mRNA levels of CYP2E1 (a) and iNOS (b) in the kidneys of rats treated with an overdose of acetaminophen. The findings are shown as mean ± standard deviations (SD). Distinct superscript letters within the same row indicate significant differences at $p < 0.05$. Abbreviations used are APAP for acetaminophen, GSEE for grape seed ethanolic extract, and PSEE for peanut skin ethanolic extract.

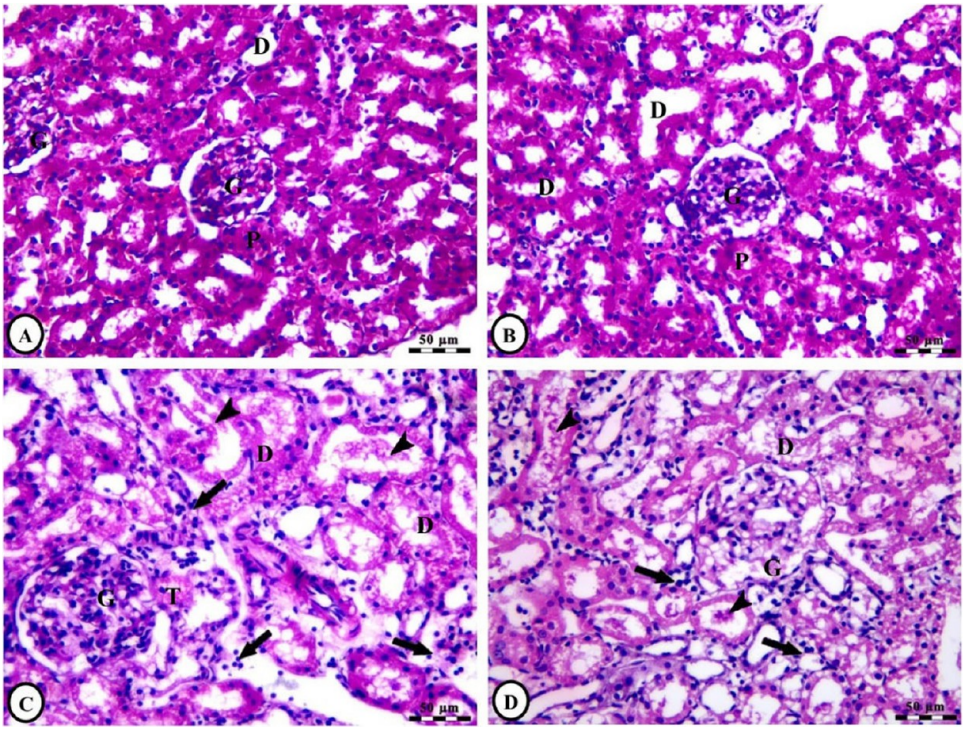

Figure 3. (A–D). Photomicrographs of renal cortex sections of rats from control and APAP groups stained with H&E (Bar = 50 μm). Photomicrographs of the renal cortex of rats from the control group show a normal structure of renal parenchyma with intact renal corpuscles containing glomeruli (G), which are surrounded with narrow Bowman's space, in addition to normal proximal (P) and distal (D) convoluted tubules (A, B). Photomicrograph of renal cortex of a rat from untreated APAP group showing severe degeneration of tubular epithelium (D), accumulation of an acidophilic proteinaceous substance in tubular lumen (arrowheads), and severe infiltration of inflammatory cells (arrows) in the renal glomeruli (G) and interstitial tissue (arrows) (C). Photomicrograph of renal cortex of another rat from untreated APAP group showing moderate necrotic glomerular epithelium (G) with enlarged Bowman's space, severe vacuolar degeneration of tubular epithelium (D), in addition to the accumulation of an acidophilic proteinaceous substance in tubular lumen (arrowheads), and severe infiltration of inflammatory cells (arrows) (D).

substantial surge ($p < 0.05$) in BWG %, with no noteworthy disparities between their received groups. No considerable impact ($p > 0.05$) of all treatments was noticed on absolute and relative kidney weights (AKW and RKW, respectively), as shown in Table 3.

3.3. Kidney Functions. Apparent disruption was noticed in kidney functions in APAP-administered rats. Serum urea and creatinine increased in APAP compared to control rats ($p < 0.05$) (Table 4). Silymarin, GSEE, and PSEE administration significantly improved these markers ($p < 0.05$) in APAP-received rats. Silymarin was so efficient that it could normalize serum creatinine concentration. No significant differences were noticed between plant extracts-received groups; however,

https://doi.org/10.1021/acsomega.4c05534
ACS Omega 2024, 9, 35154−35169

GSEE induced the same effects for both indices compared to silymarin.

3.4. Oxidative Load in Kidney Tissue Homogenate. Rat kidney tissue homogenates from different experimental groups underwent assessment for their oxidant/antioxidant status. Table 5 reveals a meaningful reduction ($p < 0.05$) in GSH levels and SOD enzyme activity in APAP compared with control. At the same time, there was a substantial increase ($p < 0.05$) in MDA and nitric oxide (NO) levels. Treatment with GSEE and PSEE alongside APAP demonstrated a significant rise of the studied antioxidants (GSH and SOD), with a considerable reduction in MDA and NO levels ($p < 0.05$) compared to the APAP-treated rats. Furthermore, the effects of these extracts were comparable to silymarin, a reference drug. Notably, there were no discernible differences between the silymarin and GSEE groups for each metric included in Table 5.

3.5. Pro-Inflammatory Cytokines in Kidney Tissue Homogenates. The pro-inflammatory cytokine profiles in kidney tissue homogenates of rats across various experimental groups. The results demonstrated a significant increase ($p < 0.05$) in TNF-α and IL-1β levels in untreated APAP-overdosed rats compared to control rats. Co-administration of either grape seed ethanol extract (GSEE) or peanut skin ethanol extract (PSEE) with APAP exhibited anti-inflammatory effects in kidney tissue, as evidenced by a considerable reduction in both TNF-α and IL-1β quantities ($p < 0.05$). Additionally, no significant differences regarding inflammation markers were observed between the silymarin-treated group, used as a reference drug, and the GSEE-treated groups, as shown in Figure 1

3.6. Renal Gene Expression. Our data exposed significant upregulation of the mRNA expression of renal iNOS and CYP2E1 in APAP-treated rats compared with the control one ($P < 0.0001$). Conversely, silymarin, GSEE, and PSEE-treated groups showed significant downregulation matching the untreated APAP group ($P < 0.0001$ for iNOS and $P < 0.001$ for CYP2E1). Silymarin normalized the mRNA expression of renal iNOS and reported no significant differences with either waste extract. As for mRNA expression of renal CYP2E1, there were insignificant differences between plant extracts-received groups. Silymarin induced a significant upregulation ($P < 0.05$) associated with the control group, while the PSEE group, rather than GSEE one, recorded a result close to that persuaded by silymarin (Figure 2).

3.7. Kidney Histopathology. Histological sections of the renal cortex in the control group illustrate a well-preserved renal architecture. These sections feature renal corpuscles with fully formed glomeruli, each bounded by a narrow Bowman's capsule, and showcase the regular appearance of both proximal and distal convoluted tubules (Figure 3a,b). An overdose of APAP induced marked pathological alterations in the renal cortex, characterized by pronounced degeneration of the tubular epithelium, deposition of an acidophilic proteinaceous material within the tubular lumen, and extensive infiltration of inflammatory cells into the renal glomeruli and interstitial areas (Figure 3c,d and Table 6). APAP-overdosed rats treated concurrently with silymarin exhibited subtle changes in the renal cortex, including slight glomerular shrinkage accompanied by expanded capsular spaces, modest degeneration of the tubular epithelium, and the presence of acidophilic proteinaceous substances within some tubular lumens. Additionally, inflammatory cell infiltration was mild in the interstitial tissue (Figure 4a,b and Table 6). Like silymarin, the plant extracts GSEE and PSEE exhibited renoprotective properties in APAP-overdosed rats. In the renal cortex of rats from the GSEE group, findings included mild glomerular shrinkage with expanded capsular spaces, moderate tubular epithelial degeneration, and localized deposits of acidophilic proteinaceous substances within some tubular lumens (Figure 4c,d and Table 6).

Table 6. Semi-Quantitative Scoring of Renal Cortex Alterations Severity in Different Treatments[a]

group alterations	control	APAP	silymarin	GSEE	PSEE
shrinkage of renal glomeruli	−	-	+	+	+
necrosis of renal glomeruli	−	++	−	-	−
tubular degeneration	−	+++	+	++	++
inflammatory cell infiltration	−	+++	+	−	−

[a]Renal cortex alterations scoring represented as (−) nil; (+) mild; (++) moderate; (+++) severe.

3.8. Molecular Docking. APAP interacted with the binding site of glutathione synthetase at the ILE401 residue (H-acceptor) with −5.23 kcal/mol (Figure 5A). Also, it is bound to the ARG144 (pi-cation) residue in the binding site of SOD1 with an energy of −4.23 kcal/mol (Figure 5B). In Figure 5C, APAP interacted by −4.37 kcal/mol energy with the GLU186 (H-donor) residue in the SOD2 binding site. Moreover, it interacted with ARG167 (H-acceptor) and VAL157 (two pi-H) residues in the SOD3's binding site with an energy of −4.71 kcal/mol (Figure 5D).

The molecular docking of silymarin and the bioactive compounds of grape seed and peanut skin extracts against TNR1A, IL1R2, Cyp2e1, and iNOS is represented in Table 7, Figures 6 and 7. Silymarin interacted with GLU108 (H-donor), GLN111 (two H-acceptors), PHE141 (H-acceptor), and ARG106 (pi-H) residues in the binding site of TNR1A at −6.70 kcal/mol (Figure 6 A). Also, it interacted by −7.46 kcal/mol with VAL67 (H-donor), GLU169 (two H-donors), ASP48 (H-donor), and ASP166 (H-acceptor) residues (Figure 6B). By H-donor (GLN358 and CYS437), H-acceptor (THR307 and GLN358), and pi-H (THR303) with the binding site of Cyp2e1 by −9.80 kcal/mol of energy (Figure 6C). By the energy of −7.96 kcal/mol, silymarin interacted with the iNOS binding site with the H-acceptor (VAL922, ALA923, and ARG959) and pi−pi (PHE1125) (Figure 6D).

Rutin, the top bioactive compound of grape seed extracts, showed higher molecular docking scores against TNR1A, IL1R2, Cyp2e1, and iNOS (Figure 7). Rutin interacted with the TNR1A binding site with THR104 (H-donor), THR123 (H-donor), LYS103 (H-acceptor), GLN111 (H-acceptor), LYS161 (H-acceptor), and HIS140 (H-pi) residues and −7.42 kcal/mol of energy (Figure 8A). By the energy of −8.06 kcal/mol, rutin bound to SER51(H-donor), VAL61 (H-donor), and LYS50 (two H-acceptors and pi-cation) residues in the binding site of IL1R2 (Figure 8B). Also, by H-donor (GLN358, THR307, and ARG435) and H-acceptor (CYS437, ALA429 (two), GLN358 (three), and THR303), rutin interacted with the binding site of Cyp2e1 by energy of −10.88 kcal/mol (Figure 7C). Moreover, rutin bound by the H-acceptor (THR926 and ARG1083) and H-pi (TYR1131) in the binding site of iNOS with an energy of −8.49 kcal/mol (Figure 7D).

3.9. Clustering Heat Map and 3D PCA Score Plot. A heat map was made to explore the connections among various treatments and variables. The cluster heat map illustrates the

https://doi.org/10.1021/acsomega.4c05534
ACS Omega 2024, 9, 35154−35169

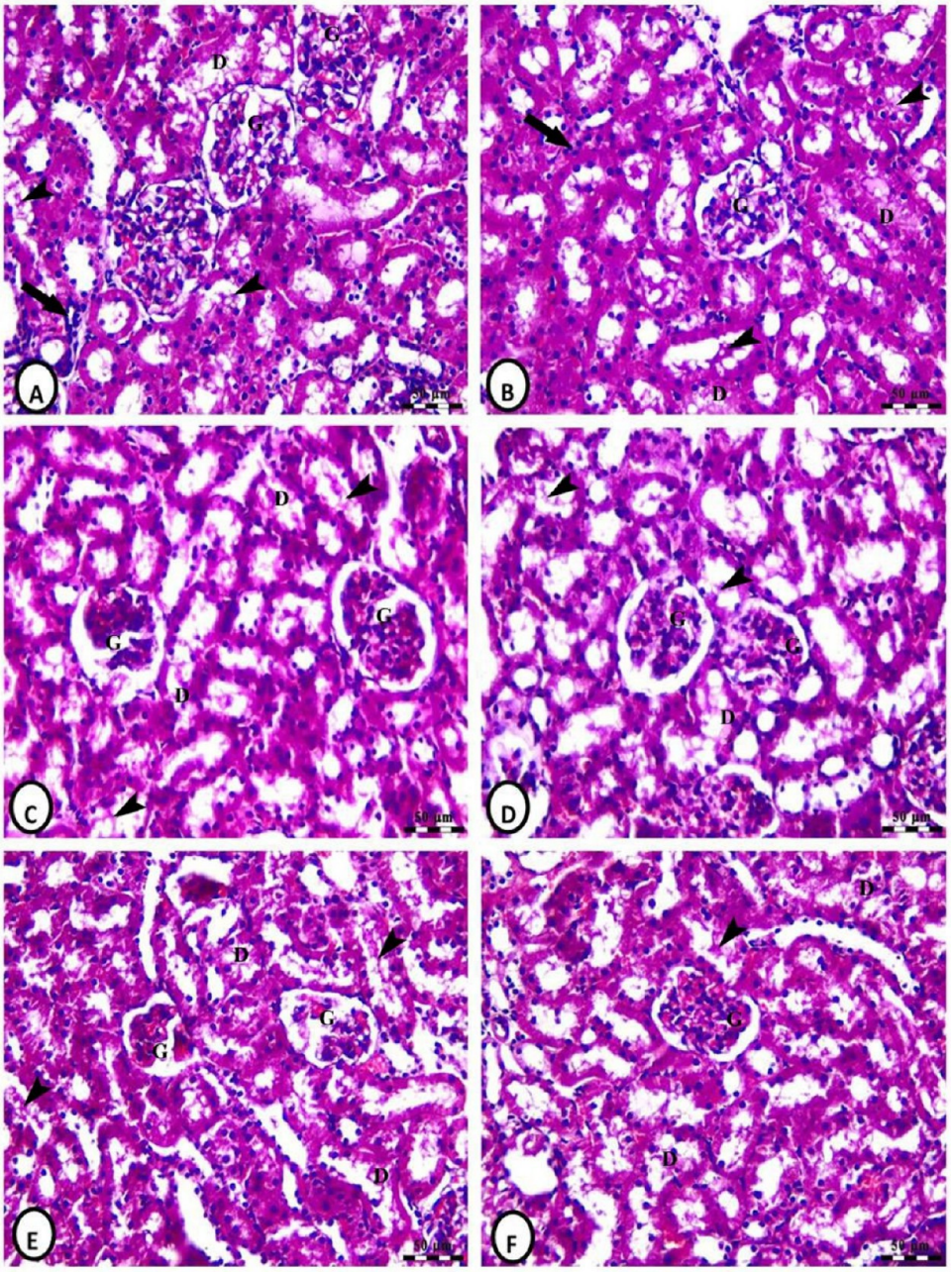

Figure 4. (A–F). Photomicrographs of renal cortex sections of rats from silymarin, GSEE, and PSEE groups stained with H&E (bar = 50 μm). Photomicrographs of the renal cortex of APAP-overdosed group concurrently treated with silymarin showed mild shrinkage of renal glomerulus (G) with wide capsular space, mild degeneration of tubular epithelium (D), and accumulation of acidophilic proteinaceous substances inside the lumen of some tubules (arrowheads), besides mild presence of inflammatory cells in the interstitial tissue (arrows) (a, b). Photomicrographs of the renal cortex of rats treated with APAP along with GSEE show mild shrinkage of the renal glomerulus (G) with wide capsular space, moderate degeneration of tubular epithelium (D), and accumulation of acidophilic proteinaceous substances inside the lumen of some tubules (arrowheads) (c, d). Photomicrographs of the renal cortex of rats treated with APAP along with PSEE showing mild shrinkage of the renal glomerulus (G) with wide capsular space, moderate degeneration, and sloughing of the tubular epithelium (D), besides the accumulation of acidophilic proteinaceous substances inside the lumen of some tubules (arrowheads) (e, f).

impact of different therapies on acetaminophen (APAP) overdose, highlighting the severity of APAP's adverse effects through dark red indicators such as urea, MDA, NO, and creatinine. Treatments like silymarin, GSEE, and PSEE display moderate improvements in these parameters, indicating their potential to counteract APAP's harmful effects. GSEE shows particular strength in reducing MDA and NO levels compared to PSEE. However, compared to silymarin, GSEE and PSEE are less effective, as seen through their higher values in harmful indicators and lower values in beneficial ones (GSH and SOD). Despite these variances, all treatments exhibit some effectiveness against APAP toxicity, with noticeable improvements in antioxidant levels (GSH and SOD) within the treated groups. The 3D PCA score plot indicates that principal component 1 (PC1) explains most of the variance at 74.54%, pointing to its significance in capturing the effects of different treatments. Groups well-separated along PC1 likely reflect distinct impacts of these treatments on the measured

https://doi.org/10.1021/acsomega.4c05534
ACS Omega 2024, 9, 35154–35169

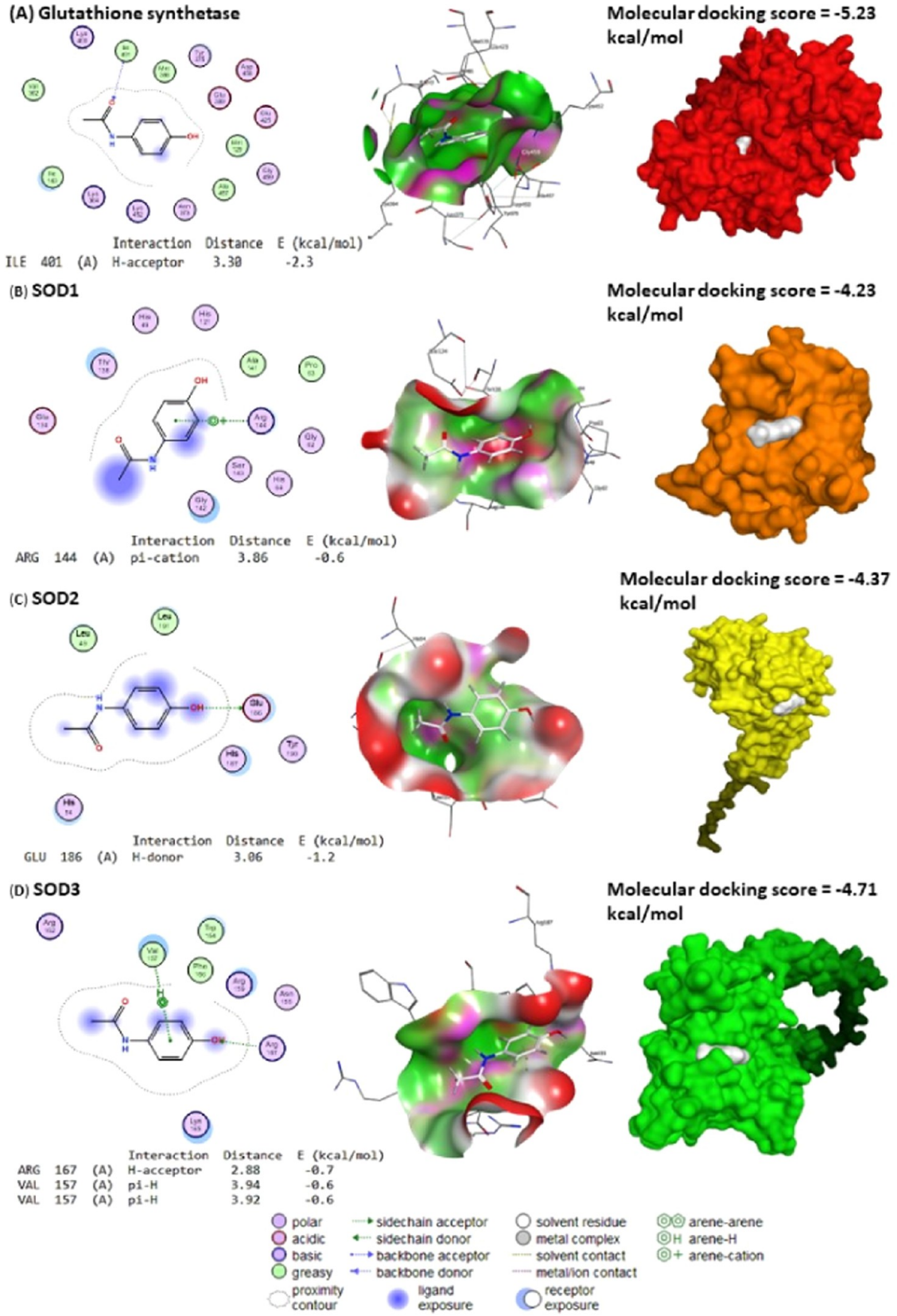

Figure 5. Molecular docking interaction of acetaminophen (APAP) against glutathione synthetase, superoxide dismutase (SOD1), SOD2, and SOD3.

parameters. The closer proximity of GSEE and PSEE groups to the control group, as opposed to the APAP group, suggests

https://doi.org/10.1021/acsomega.4c05534
ACS Omega 2024, 9, 35154−35169

Table 7. Molecular Docking Analysis of Silymarin and Active Ingredients in Grape Seed and Peanut Skin Extracts Targeting TNR1A, IL1R2, Cyp2e1, and iNOS

		molecular docking scores (kcal/mol)			
	compounds	TNR1A	IL1R2	Cyp2e1	iNOS
extracts' bioactive compounds	silymarin	−6.70	−7.46	−9.80	−7.96
	apigenin-7-glucoside	−6.43	−7.24	−9.10	−6.68
	caffeic acid	−4.27	−5.61	−5.74	−4.96
	catechin	−5.07	−5.94	−6.93	−5.91
	chlorogenic acid	−5.66	−6.22	−8.03	−6.01
	chrysin	−4.81	−5.73	−6.77	−6.24
	cinnamic acid	−4.46	−5.10	−5.29	−5.03
	ferulic acid	−4.76	−5.50	−5.84	−5.09
	gallic acid	−4.02	−4.83	−5.38	−4.78
	gentisic acid	−4.57	−4.70	−5.12	−4.67
	p-coumaric acid	−4.27	−5.14	−5.44	−5.22
	p-hydroxybenzoic	−4.20	−4.77	−4.92	−4.33
	protocatechuic acid	−4.19	−4.58	−5.14	−4.67
	quercetin	−5.19	−5.78	−7.05	−5.71
	rosmarinic acid	−5.59	−7.10	−7.86	−6.89
	rutin	−7.42	−8.06	−10.88	−8.49
	sinapinic acid	−4.83	−5.88	−6.28	−5.27
	syringic acid	−4.45	−5.47	−6.08	−5.47
	vanillic acid	−4.15	−5.33	−5.75	−4.68

that these treatments may mitigate the APAP-induced alterations with a return toward normal parameter levels (Figure 8A,B).

4. DISCUSSION

Acetaminophen, APAP, is widely used worldwide.[6] This medication is both safe and effective in the prescribed amounts. However, it has the potential to cause kidney damage. Overdose is associated with numerous health problems.[2] The search for new, safe interventions as dietary sources that can face the mechanisms of APAP's toxic actions is ultimately needed. The existing study analyzed the renoprotective effects of grape seeds and peanut skin ethanolic extracts (GSEE and PSEE) vs silymarin in APAP-overdosed rats.

Herein, the identification trial of the phenolic profile of both extracts by HPLC revealed the presence of catechin and gallic acid at significant concentrations in GSEE. In contrast, protocatechuic acid, rutin, *p*-hydroxybenzoic acid, and apigenin-7-glucoside were found in small amounts. In PSEE, the majority was for catechin, followed by protocatechuic, *p*-coumaric, and gallic acids, while apigenin-7-glucoside, caffeic acid, rosmarinic acid, and ferulic acid were retrieved at medium concentrations. These phenolic compounds were reported to exert renoprotective actions through their potential antioxidant, anti-inflammatory, and mitochondrial protecting consequences. In this regard, Wongmekiat et al.[49] demonstrated the effectiveness of catechin in protecting the kidney against cadmium toxicity. Gallic and protocatechuic acids were also reported to prevent cisplatin and doxorubicin-induced nephrotoxicity in rats, respectively,[50] while in renal ischemia/reperfusion animal models, rutin, caffeic acid, and *p*-coumaric acid were able to prevent renal insufficiency.[51] Similarly, the findings of El-Desouky et al.[52] suggested substances high in rosmarinic acid as a means to avoid kidney toxicity, remarkably for individuals who are more vulnerable to drug intoxication, environmental contaminants, and toxins. Moreover, De et al.[53] referred to apigenin-7-glucoside as a reference therapeutic agent for treating oxalate-mediated renal injury and nephrolithiasis.

However, the present results indicate the weight gain %—losing the impact of APAP overdose. This result was supported by Adeneye and Olagunju,[54] who related this effect to the greater urinary volume. However, silymarin and GSEE lessened this increase in urinary volume, which may account for the significant weight gain recorded for the groups that received them. This hypothesis needs more validation.

This dramatic rise in creatinine and urea levels demonstrated, in this investigation, that APAP overdose-induced renal dysfunction and nephrotoxicity as nitrogen wastes in serum were in harmony with many studies that suggested increased oxidative stress and inflammation outputs as main and intermediate promoters.[2,55] In renal diseases, urea, and creatinine accumulate in serum not because of intensified production but because of a decreased clearance rate, indicating a defect in renal function.[56]

Kidney damage from acetaminophen (APAP) toxicity involves multiple pathways. One key mechanism is the microsomal enzyme cytochrome P450, particularly CYP2E1 found in the kidney, which is more active in males, linking nephrotoxicity to gender.[4] Another pathway involves prostaglandin endoperoxide synthetase (PGES) in the kidneys, which converts APAP into harmful metabolites like NAPQI, more so in the renal medulla. In the renal cortex, cytochrome P450 predominates. Overproduction of NAPQI, especially after an overdose and insufficient glutathione, leads to protein dysfunction and cellular death.[57]

The enzyme *N*-deacetylase is implicated in acetaminophen (APAP)-induced kidney toxicity, although its exact function is not fully understood. It is recognized for its ability to deacetylate APAP or its toxic metabolite NAPQI, transforming it into *p*-aminophenol. This intermediate is then converted into a free radical that can attach to cellular proteins, suggesting a possible synergy with the cytochrome P450 (CYP-450) enzyme system's actions. This mechanism has been documented in various animal studies.[58]

https://doi.org/10.1021/acsomega.4c05534
ACS Omega 2024, 9, 35154−35169

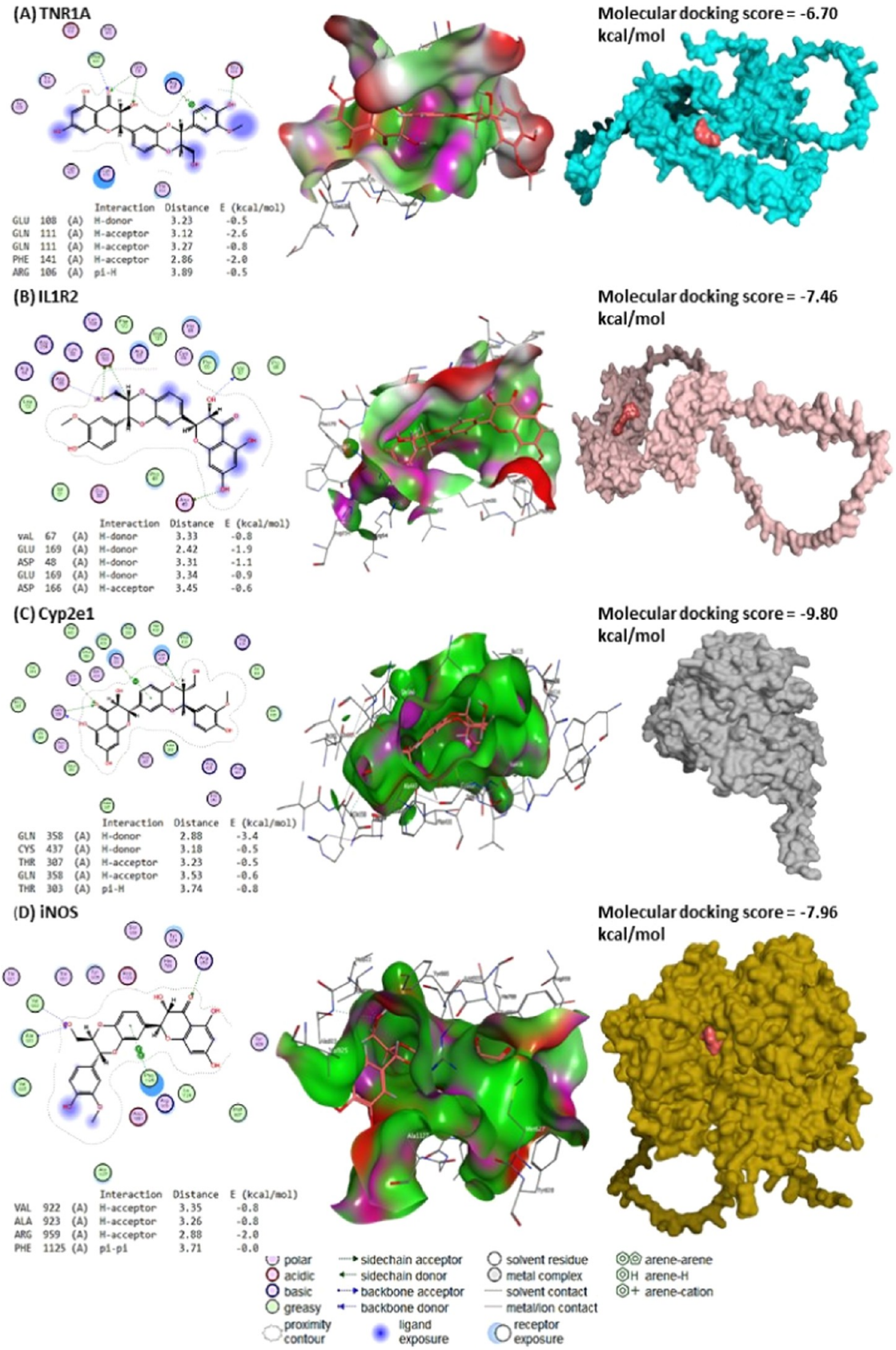

Figure 6. Interaction analysis through molecular docking of silymarin with (TNR1A, IL1R2, Cyp2e1) and iNOS.

ROS are associated with oxidative stress, which is linked to several anomalies such as diabetes, cancer, heart disease, and liver and kidney damage.[59] The relationship between ROS and internal enzymatic and nonenzymatic antioxidants, such as GSH, SOD, and others like CAT and GPx, is essential. It may be a critical defense against oxidative stress-related injuries. It is

https://doi.org/10.1021/acsomega.4c05534
ACS Omega 2024, 9, 35154−35169

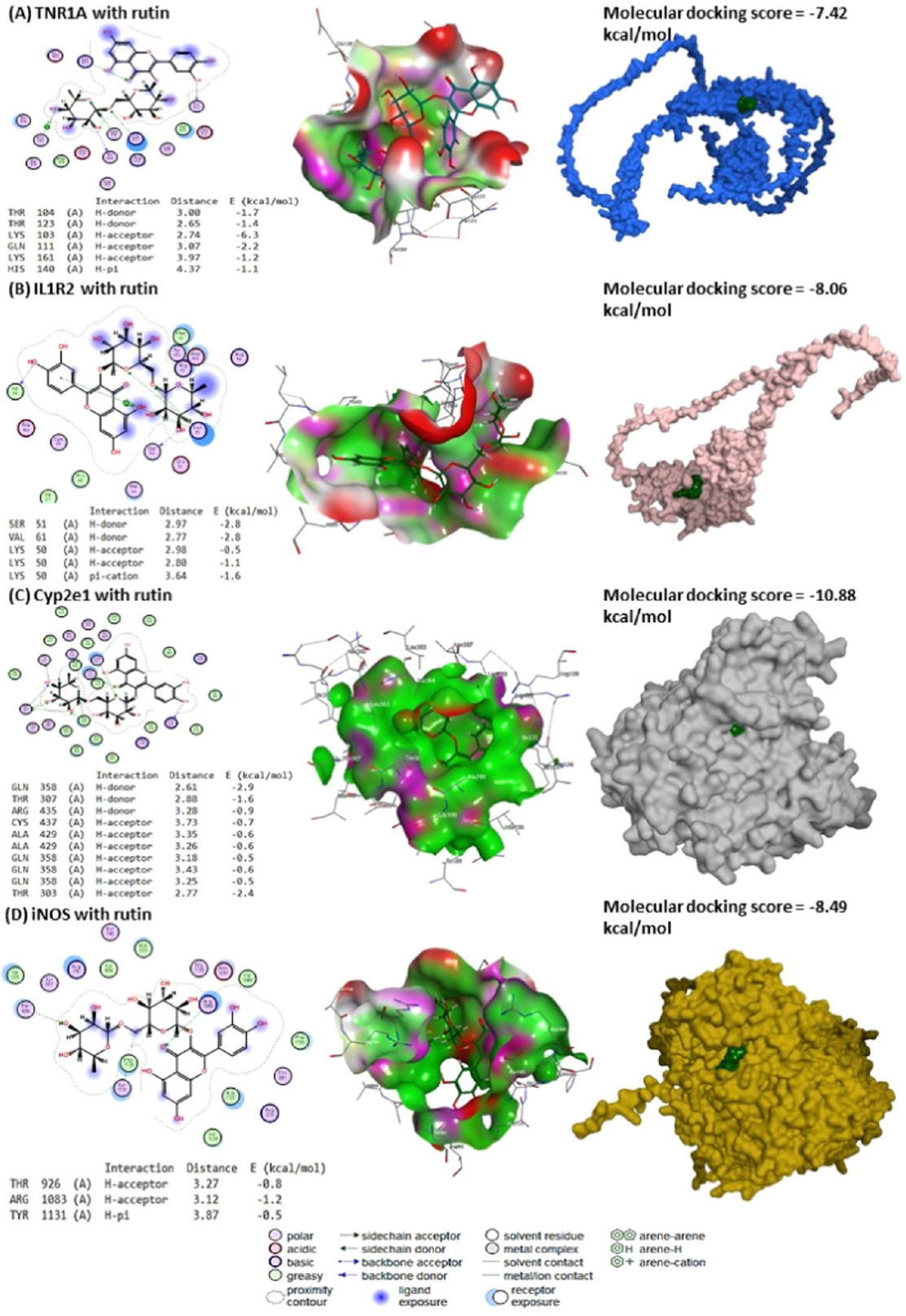

Figure 7. Molecular docking interaction of rutin from GSEE against TNR1A, IL1R2, Cyp2e1, and iNOS.

commonly known that APAP-induced toxicity resulted in decreased amounts or activities of internal antioxidants vs a marked elevation in lipid peroxidation process rate.[2,60] On the other hand, the findings of Mohamed et al.[61] exhibited an elevation of nitric oxide concentration in AKI induced by paracetamol exposure. These previous studies strongly supported the current findings.

Moreover, paracetamol at the used dose (640 mg/kg body weight/day) promoted inflammation obviously, evidenced through the noticed increase in levels of TNF-α and IL-1β

https://doi.org/10.1021/acsomega.4c05534
ACS Omega 2024, 9, 35154−35169

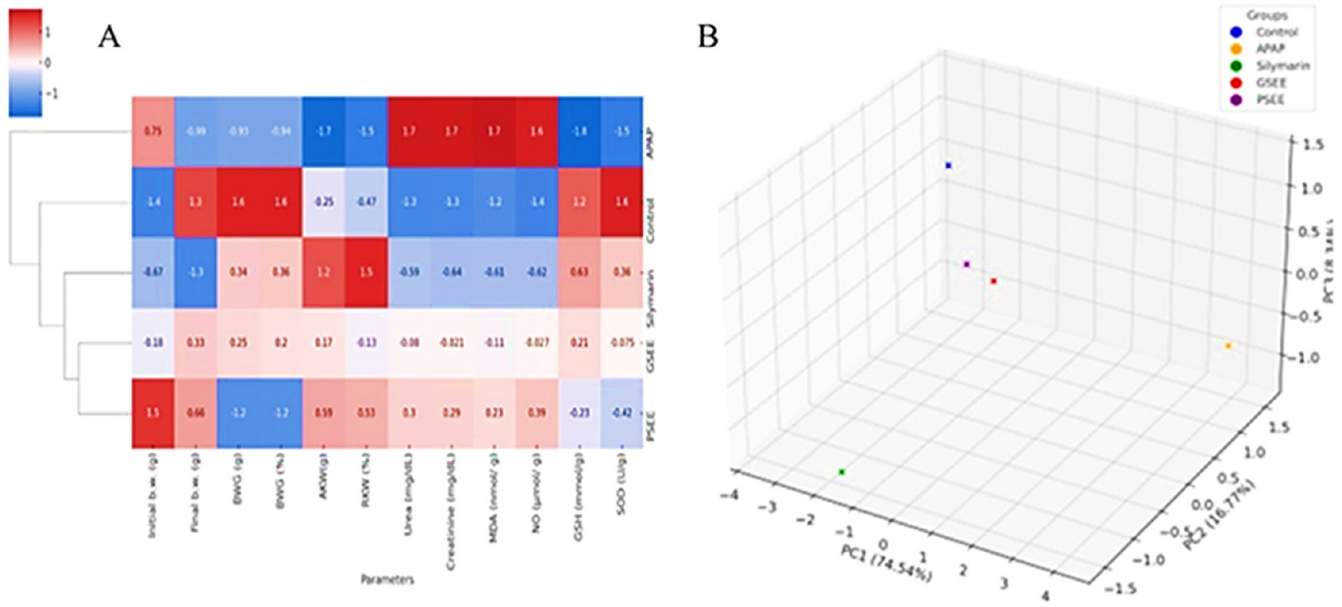

Figure 8. (A) The clustering heat map represents all data sets, where each color-coded cell indicates concentration levels, organizing variable averages by columns and treatment by rows. On the gradient scale, dark red signifies the highest concentration, while blue marks the lowest. (B) 3D score plot of PCA for discerning the experiment groups.

in kidney homogenates, which was in line with many previous studies.[62] This can be attributed to an increased ROS production. ROS can promote an inflammatory response by activating nuclear factor-kappa B, which controls gene expression in tissue damage and inflammation.[63] Also, molecular docking assessment revealed the inhibitory effect of APAP against glutathione synthetase, SOD1, SOD2, and SOD3, leading to a reduction in the cellular antioxidant potential.

However, a gene expression assay showed that rat exposure to PCM overdose reported a highly significant upregulation of the mRNA expression of both renal INOS and CYP2E1. These results approved the harmful effects of PCM. They assured the above mechanistic insights into the ability of the drug overdose to enhance nitric oxide synthesis, as well as the promoted role of the CYP-450 isoenzyme, CYP2E1, in PCM-induced AKI. In the study of Aksun et al.,[64] immunohistochemical staining proved that APAP boosted iNOS activity, suggesting oxidative injury in the kidneys and liver.

Herein, the renal cortex sections of rats in which an overdose of APAP was applied showed many abnormal histological changes, which were in harmony with those indicated by many previous experimental studies.[2,65] The APAP's ability to improve ROS and pro-inflammatory cytokine production, as shown above, is how it causes these kidney structural abnormalities.

In the present study, silymarin, GSEE, and PSEE demonstrated enhanced antioxidant and anti-inflammatory mechanisms in kidney tissue homogenates, improving serum nitrogen waste levels. Additionally, they effectively regulated the expression of mRNA of the studied renal genes (INOS and CYP2E1), resulting in the resolution of structural abnormalities. Numerous investigations utilizing diverse models of renal toxicity[66] rather than acetaminophen[67] have further emphasized the preventive attributes of silymarin.

These studies provided valuable mechanistic insights into the renoprotective effects of silymarin. It was opined that silymarin accumulates in kidney cells, contributing to repair and regeneration by enhancing protein and nucleic acid synthesis,[68] attributed to silybin and silychristin, two essential components of silymarin. Of them, silybin only represents 50% of the silymarin structure and has been considered the most prominent bioactive.[69] In this regard, silymarin's antioxidant and anti-inflammatory properties are significantly implicated.

According to this study, GSEE was the closest treatment to silymarin. Many animal studies also cited grape seed extracts' renoprotective and antiurolithic effects.[70] Phenolic compounds in grape seeds function as antioxidants by donating hydrogen and electrons and stabilizing radical intermediates to prevent oxidation. Procyanidin B1, found in grape seed extracts, is particularly effective at scavenging and killing radicals. Additionally, proanthocyanidins in grape seed extract safeguard the sulfhydryl groups in glutathione from oxidative harm.[71] Furthermore, grape seed proanthocyanidins have demonstrated the ability to combat oxidative injury by influencing metabolic functions, improving detoxification pathways and averting xenobiotic interactions with biological molecules.[72]

Besides, grape seed phytochemicals were found to induce anti-inflammatory and lipid-lowering effects.[73] PSEE caused its protective effects to be in the same range as the APAP group. Its nephroprotective action was referenced.[74]

Yang et al.[14] demonstrated that peanut skin extract (PSE) effectively ameliorates kidney damage in rats on a high-fat and high-fructose diet by reducing kidney tissue, perinephric fat weight, and serum ammonia, urea nitrogen, and creatinine levels. Additionally, PSE significantly decreased renal concentrations of TNF-α and IL-1β. Histopathological evaluations showed that PSE alleviated renal tubular dilatation, degeneration, and partial sloughing off of tubular epithelial cells. It also diminished serum and urinary uric acid levels and decreased the production and activity of xanthine oxidase in both the serum and liver. Furthermore, PSE suppressed the renal expression of the NLRP3 inflammasome and proteins associated with endoplasmic reticulum stress. In silico analyses revealed that silymarin, along with the active components of grape seeds and peanut skins, effectively inhibited TNR1A,

https://doi.org/10.1021/acsomega.4c05534
ACS Omega 2024, 9, 35154−35169

IL1R2, Cyp2e1, and iNOS, showcasing their potential to mitigate the inflammatory response triggered by APAP.

The phenolic and flavonoid compounds and other bioactive components were generally suggested to possess antioxidant properties in food products enriched with these byproducts. Furthermore, they hinted at many medicinal and biological actions, such as anti-inflammatory and antioxidation effects.[75]

5. CONCLUSIONS

This study demonstrates the potential of ethanolic extracts from grape seeds (GSEE) and peanut skins (PSEE) in protecting against acute kidney injury induced by an acetaminophen (APAP) overdose. Both extracts significantly reduced the harmful effects of APAP, such as increased serum urea and creatinine levels, decreased body weight gain, and elevated levels of oxidative stress and inflammatory markers. GSEE showed efficacy similar to that of silymarin, a known therapeutic agent. Molecular docking studies supported these findings by showing that compounds in GSEE and PSEE inhibited key enzymes and receptors involved in inflammation and oxidative stress. These results suggest that GSEE and PSEE could be viable alternatives for treating APAP-induced kidney damage, warranting further research to isolate and identify their effective compounds.

■ ASSOCIATED CONTENT

Data Availability Statement

The data underlying this study are available in the published article and its Supporting Information.

Supporting Information

The Supporting Information is available free of charge at https://pubs.acs.org/doi/10.1021/acsomega.4c05534.

The HPLC analysis of the GSEE (Figure S1); the phenolic profile of the GSEE (Table S1); the HPLC analysis of the PSEE (Figure S2); the phenolic profile of the PSEE (Table S2) (PDF)

■ AUTHOR INFORMATION

Corresponding Authors

Samy M. Sayed − *Department of Science and Technology, University College-Ranyah, Taif University, Taif 21944, Saudi Arabia*; Email: samy_mahmoud@hotmail.com

Mustafa Shukry − *Department of Physiology, Faculty of Veterinary Medicine, Kafrelsheikh University, Kafrelsheikh 33516, Egypt*; orcid.org/0000-0003-2722-2466; Email: mostafa.ataa@vet.kfs.edu.eg

Authors

Samah A. El-Hashash − *Department of Nutrition and Food Science, Faculty of Home Economics, Al-Azhar University, Tanta City 31732, Egypt*

Wafaa A. Gaballah − *Department of Nutrition and Food Science, Faculty of Home Economics, Al-Azhar University, Tanta City 31732, Egypt*

Asmaa Antar Faramawy − *Department of Nutrition and Food Science, Faculty of Home Economics, Al-Azhar University, Tanta City 31732, Egypt*

Nermin I. Rizk − *Medical Physiology Department, Faculty of Medicine, Menoufia University, Shebin el Kom 32511, Egypt*

Meshari A. Alsuwat − *Department of Clinical Laboratory Sciences, College of Applied Medical Sciences, Taif University, Taif 21944, Saudi Arabia*

Mohammed Ali Alshehri − *Department of Biology, Faculty of Science, University of Tabuk, Tabuk 47512, Saudi Arabia*

Complete contact information is available at: https://pubs.acs.org/10.1021/acsomega.4c05534

Author Contributions

S.A.E.-H., W.A.G., and A.A.F. supervised and performed experiments; N.I.R., M.Ali.A., and M.A.A. designed the experiments; S.M.S., M.S., M.Ali.A, and M.A.A. analyzed data and wrote and finalized the manuscript; S.A.E.-H., W.A.G., N.I.R., and A.A.F. wrote, interpreted data, and finalized the manuscript.

Notes

The authors declare no competing financial interest.

■ ACKNOWLEDGMENTS

The authors express gratitude toward the Department of Nutrition and Food Science at the Faculty of Home Economics, Al-Azhar University, for providing nonfinancial resources necessary to complete this study. The authors extend their appreciation to Taif University, Saudi Arabia, for supporting this work through project number (TU-DSPP-2024-22).

■ REFERENCES

(1) Fisher, E. S.; Curry, S. C. Evaluation and treatment of acetaminophen toxicity. *Adv. Pharmacol.* **2019**, *85*, 263−272.

(2) Reshi, M. S.; Shrivastava, S.; Jaswal, A.; Sinha, N.; Uthra, C.; Shukla, S. Gold nanoparticles ameliorate acetaminophen induced hepato-renal injury in rats. *Exp. Toxicol. Pathol.* **2017**, *69* (4), 231−240.

(3) Khan, Z.; Abumedian, M.; Ibekwe, M.; Musa, K.; Mlawa, G. Acute renal impairment in patients due to paracetamol overdose in the absence of hepatic impairment. *Cureus* **2021**, *13* (12), No. e20727, DOI: 10.7759/cureus.20727.

(4) Mazer, M.; Perrone, J. Acetaminophen-induced nephrotoxicity: pathophysiology, clinical manifestations, and management. *J. Med. Toxicol.* **2008**, *4*, 2−6.

(5) Mostafa, E. M.; Tawfik, A. M.; Abd-Elrahman, K. M. Egyptian perspectives on potential risk of paracetamol/acetaminophen-induced toxicities: Lessons learnt during COVID-19 pandemic. *Toxicol. Rep.* **2022**, *9*, 541−548.

(6) Saccomano, S. J. Acute acetaminophen toxicity in adults. *Nurs. Crit. Care* **2019**, *14* (5), 10−17.

(7) El-Boshy, M.; BaSalamah, M. A.; Ahmad, J.; Idris, S.; Mahbub, A.; Abdelghany, A. H.; Almaimani, R. A.; Almasmoum, H.; Ghaith, M. M.; Elzubier, M.; Refaat, B. Vitamin D protects against oxidative stress, inflammation and hepatorenal damage induced by acute paracetamol toxicity in rat. *Free Radical Biol. Med.* **2019**, *141*, 310−321.

(8) Cabello-Verrugio, C.; Simon, F.; Trollet, C.; Santibañez, J. F. Oxidative stress in disease and aging: mechanisms and therapies 2016. *Oxid. Med. Cell. Longevity* **2016**, *2017*, No. 4310469.

(9) Khazaei, R.; Seidavi, A.; Bouyeh, M. A review on the mechanisms of the effect of silymarin in milk thistle (Silybum marianum) on some laboratory animals. *Vet. Med. Sci.* **2022**, *8* (1), 289−301.

(10) Georgiev, T.; Nikolova, G.; Dyakova, V.; Karamalakova, Y.; Georgieva, E.; Ananiev, J.; Ivanov, V.; Hadzhibozheva, P. Vitamin E and Silymarin Reduce Oxidative Tissue Damage during Gentamycin-Induced Nephrotoxicity. *Pharmaceuticals* **2023**, *16* (10), 1365.

(11) Osuntokun, O. S.; Olayiwola, G.; Atere, T. G.; Adedokun, K. I.; Oladokun, O. O. Graded doses of grape seed methanol extract attenuated hepato-toxicity following chronic carbamazepine treatment in male Wistar rats. *Toxicol. Rep.* **2020**, *7*, 1592−1596.

(12) Yun, S.; Chu, D.; He, X.; Zhang, W.; Feng, C. Protective effects of grape seed proanthocyanidins against iron overload-induced renal oxidative damage in rats. *J. Trace Elem. Med. Biol.* **2020**, *57*, No. 126407.
(13) Makau, J. N.; Watanabe, K.; Mohammed, M. M.; Nishida, N. Antiviral activity of peanut (Arachis hypogaea L.) skin extract against human influenza viruses. *J. Med. Food* **2018**, *21* (8), 777−784.
(14) Yang, Y.; Yu, J.; Huo, J.; Yang, L.; Yan, Y. Protective effects of peanut skin extract on high-fat and high-fructose diet-induced kidney injury in rats. *Food Sci. Biotechnol.* **2023**, *32*, 1−9.
(15) Ho-Ting Shiu, P.; Zheng, C.; Rangsinth, P.; Wang, W.; Li, J.; Li, R.; Pak-Heng Leung, G. Anti-inflammatory effect of gallic acid on HaCaT keratinocytes through the inhibition of MAPK-, NF-κB-, and Akt-dependent signaling pathways. *Bangladesh J. Pharmacol.* **2022**, *17* (4), No. 24.
(16) Zhou, C.; Ao, H.-Y.; Han, X.; Jiang, W.-W.; Yang, Z.-F.; Ma, L.; Deng, X.-Y.; Wan, Y.-Z. Engineering a novel antibacterial agent with multifunction: Protocatechuic acid-grafted-quaternized chitosan. *Carbohydr. Polym.* **2021**, *258*, No. 117683.
(17) Zhang, J.; Li, D.-M.; Sun, W.-J.; Wang, X.-J.; Bai, J.-G. Exogenous p-hydroxybenzoic acid regulates antioxidant enzyme activity and mitigates heat stress of cucumber leaves. *Sci. Hortic.* **2012**, *148*, 235−245.
(18) Joshi, R.; Gangabhagirathi, R.; Venu, S.; Adhikari, S.; Mukherjee, T. Antioxidant activity and free radical scavenging reactions of gentisic acid: in-vitro and pulse radiolysis studies. *Free Radical Res.* **2012**, *46* (1), 11−20.
(19) Ganeshpurkar, A.; Saluja, A. The pharmacological potential of catechin. *Indian J. Biochem. Biophys.* **2020**, *57* (5), 505−511.
(20) Ong, K. W.; Hsu, A.; Tan, B. K. H. Anti-diabetic and anti-lipidemic effects of chlorogenic acid are mediated by ampk activation. *Biochem. Pharmacol.* **2013**, *85* (9), 1341−1351.
(21) Silva, T.; Oliveira, C.; Borges, F. Caffeic acid derivatives, analogs and applications: A patent review (2009−2013). *Expert Opin. Ther. Pat.* **2014**, *24* (11), 1257−1270.
(22) Srinivasulu, C.; Ramgopal, M.; Ramanjaneyulu, G.; Anuradha, C.; Kumar, C. S. Syringic acid (SA)—a review of its occurrence, biosynthesis, pharmacological and industrial importance. *Biomed. Pharmacother.* **2018**, *108*, 547−557.
(23) Deng, J.-S.; Chang, Y.-C.; Wen, C.-L.; Liao, J.-C.; Hou, W.-C.; Amagaya, S.; Huang, S.-S.; Huang, G.-J. Hepatoprotective effect of the ethanol extract of Vitis thunbergii on carbon tetrachloride-induced acute hepatotoxicity in rats through anti-oxidative activities. *J. Ethnopharmacol.* **2012**, *142* (3), 795−803.
(24) Zduńska, K.; Dana, A.; Kolodziejczak, A.; Rotsztejn, H. Antioxidant properties of ferulic acid and its possible application. *Skin Pharmacol. Physiol.* **2018**, *31* (6), 332−336.
(25) Chen, C. Sinapic acid and its derivatives as medicine in oxidative stress-induced diseases and aging. *Oxid. Med. Cell. Longevity* **2016**, *2016*, No. 3571614, DOI: 10.1155/2016/3571614.
(26) Sthijns, M. M.; Schiffers, P. M.; Janssen, G. M.; Lemmens, K. J.; Ides, B.; Vangrieken, P.; Bouwman, F. G.; Mariman, E. C.; Pader, I.; Arnér, E. S.; et al. Rutin protects against H2O2-triggered impaired relaxation of placental arterioles and induces Nrf2-mediated adaptation in Human Umbilical Vein Endothelial Cells exposed to oxidative stress. *Biochim. Biophys. Acta, Gen. Subj.* **2017**, *1861* (5), 1177−1189.
(27) Amalan, V.; Vijayakumar, N.; Ramakrishnan, A. p-Coumaric acid regulates blood glucose and antioxidant levels in streptozotocin induced diabetic rats. *J. Chem. Pharm. Res.* **2015**, *7* (7), 831−839.
(28) Salehi, B.; Venditti, A.; Sharifi-Rad, M.; Kręgiel, D.; Sharifi-Rad, J.; Durazzo, A.; Lucarini, M.; Santini, A.; Souto, E. B.; Novellino, E.; et al. The therapeutic potential of apigenin. *Int. J. Mol. Sci.* **2019**, *20* (6), 1305.
(29) Adomako-Bonsu, A. G.; Chan, S. L.; Pratten, M.; Fry, J. R. Antioxidant activity of rosmarinic acid and its principal metabolites in chemical and cellular systems: Importance of physico-chemical characteristics. *Toxicol. In Vitro* **2017**, *40*, 248−255.
(30) Song, F.; Li, H.; Sun, J.; Wang, S. Protective effects of cinnamic acid and cinnamic aldehyde on isoproterenol-induced acute myocardial ischemia in rats. *J. Ethnopharmacol.* **2013**, *150* (1), 125−130.
(31) Lesjak, M.; Beara, I.; Simin, N.; Pintać, D.; Majkić, T.; Bekvalac, K.; Orčić, D.; Mimica-Dukić, N. Antioxidant and anti-inflammatory activities of quercetin and its derivatives. *J. Funct. Foods* **2018**, *40*, 68−75.
(32) Farkhondeh, T.; Abedi, F.; Samarghandian, S. Chrysin attenuates inflammatory and metabolic disorder indices in aged male rat. *Biomed. Pharmacother.* **2019**, *109*, 1120−1125.
(33) Vargas-Mendoza, N.; Madrigal-Santillán, E.; Morales-González, Á.; Esquivel-Soto, J.; Esquivel-Chirino, C.; y González-Rubio, M. G.-L.; Gayosso-de-Lucio, J. A.; Morales-González, J. A. Hepatoprotective effect of silymarin. *World J. Hepatol.* **2014**, *6* (3), 144.
(34) Kim, K.-H.; Tsao, R.; Yang, R.; Cui, S. W. Phenolic acid profiles and antioxidant activities of wheat bran extracts and the effect of hydrolysis conditions. *Food Chem.* **2006**, *95* (3), 466−473.
(35) Ucar, F.; Taslipinar, M. Y.; Alp, B. F.; Aydin, I.; Aydin, F. N.; Agilli, M.; Toygar, M.; Ozkan, E.; Macit, E.; Oztosun, M.; et al. The effects of N-acetylcysteine and ozone therapy on oxidative stress and inflammation in acetaminophen-induced nephrotoxicity model. *Renal Failure* **2013**, *35* (5), 640−647.
(36) Islam, M. T.; Quispe, C.; Islam, M. A.; Ali, E. S.; Saha, S.; Asha, U. H.; Mondal, M.; Razis, A. F. A.; Sunusi, U.; Kamal, R. M.; et al. Effects of nerol on paracetamol-induced liver damage in Wistar albino rats. *Biomed. Pharmacother.* **2021**, *140*, No. 111732.
(37) Fuadiyah, D.; Kurniawan, I. Effect of Peanut Shell Extract (Arachis hypogaea L.) on Osteoclasts in Alveolar Bone of Wistar Rats induced by Aggregatibacter actinomycetemcomitans. *Malays. J. Med. Res.* **2021**, *17*, No. 28.
(38) Abd Eldaim, M. A.; Barakat, E. R.; Alkafafy, M.; Elaziz, S. A. A. Antioxidant and anti-apoptotic prophylactic effect of silymarin against lead-induced hepatorenal toxicity in rats. *Environ. Sci. Pollut. Res.* **2021**, *28* (41), 57997−58006.
(39) Özden, F. O.; Sakallioğlu, E. E.; Sakallioğlu, U.; Ayas, B.; Erişgin, Z. Effects of grape seed extract on periodontal disease: An experimental study in rats. *J. Appl. Oral Sci.* **2017**, *25* (2), 121−129.
(40) Baskaran, K.; Suruthi, B. Hepatoprotective activity of ethanolic seed extract of Lawsonia inermis against paracetamol-induced liver damage in rats. *Sch. J. Appl. Med. Sci.* **2016**, *4* (7), 2488−2491.
(41) Angervall, L.; Carlström, E. Theoretical criteria for the use of relative organ weights and similar ratios in biology. *J. Theor. Biol.* **1963**, *4* (3), 254−259.
(42) Patton, C. J.; Crouch, S. Spectrophotometric and kinetics investigation of the Berthelot reaction for the determination of ammonia. *Anal. Chem.* **1977**, *49* (3), 464−469.
(43) Houot, O. Kinetic Determination of Creatinine. In *Interpretation of Clinical Laboratory Tests*; Henny, J.; Henny, J.; Siest, G.; Schiele, F.; Young, D. S., Eds.; Biomedical Publications, 1985.
(44) Ohkawa, H.; Ohishi, N.; Yagi, K. Assay for lipid peroxides in animal tissues by thiobarbituric acid reaction. *Anal. Biochem.* **1979**, *95* (2), 351−358.
(45) Miranda, K. M.; Espey, M. G.; Wink, D. A. A rapid, simple spectrophotometric method for simultaneous detection of nitrate and nitrite. *Nitric Oxide* **2001**, *5* (1), 62−71.
(46) Ellman, G. L. Tissue sulfhydryl groups. *Arch. Biochem. Biophys.* **1959**, *82*, 70−77. Misra, H. P.; Fridovich, I. The role of superoxide anion in the autoxidation of epinephrine and a simple assay for superoxide dismutase. *J. Biol. Chem.* **1972**, *247* (10), 3170−3175.
(47) Theakston, R. D. G.; Warrell, D.; Griffiths, E. Report of a WHO workshop on the standardization and control of antivenoms. *Toxicon* **2003**, *41* (5), 541−557.
(48) Bancroft, J. D.; Layton, C. The Hematoxylins and Eosin. In *Bancroft's Theory and Practice of Histological Techniques*; Elsevier, 2012; Vol. 7, pp 173−186.
(49) Wongmekiat, O.; Peerapanyasut, W.; Kobroob, A. Catechin supplementation prevents kidney damage in rats repeatedly exposed

to cadmium through mitochondrial protection. *Naunyn Schmiedebergs Arch. Pharmacol.* **2018**, *391*, 385−394.
(50) Obafemi, T. O.; Anyalechi, D. I.; Afolabi, B. A.; Ekundayo, B. E.; Adewale, O. B.; Afolabi, O. B.; Anadozie, S. O.; Olaoye, O. A.; Adu, I. A.; Onasanya, A. Nephroprotective effects of gallic acid and hesperidin in aluminum chloride-induced toxicity in rats. *Phytomed. Plus* **2022**, *2* (4), No. 100378.
(51) Mozaffari Godarzi, S.; Gorji, A. V.; Gholizadeh, B.; Mard, S. A.; Mansouri, E. Antioxidant effect of p-coumaric acid on interleukin 1-β and tumor necrosis factor-α in rats with renal ischemic reperfusion. *Nefrologia* **2020**, *40* (3), 311−319.
(52) El-Desouky, M. A.; Mahmoud, M. H.; et al. Nephroprotective effect of green tea, rosmarinic acid and rosemary on N-diethylnitrosamine initiated and ferric nitrilotriacetate promoted acute renal toxicity in Wistar rats. *Interdiscip. Toxicol.* **2019**, *12* (2), 98.
(53) De, L.; Qianlin, S.; Ziqi, H.; Chang, S.; Shengming, J.; Caitao, D.; Sixing, Y. Repairing effect of apigenin-7-glucoside on oxalate-mediated HK-2 cell damage via the lRE1/ASK1/P38 MAPK pathway. *J. Clin. Urol.* **2022**, *37* (6), 440−446.
(54) Adeneye, A.; Olagunju, J. Protective effect of oral ascorbic acid (Vitamin C) on acetaminophen-induced renal injury in rats. *Afr. J. Biomed. Res.* **2009**, *12* (1), 55−61.
(55) Wei, M.; Gao, Y.; Cheng, D.; Zhang, H.; Zhang, W.; Shen, Y.; Huang, Q.; An, X.; Wang, B.; Yu, Z.; et al. Notoginsenoside Fc ameliorates renal tubular injury and mitochondrial damage in acetaminophen-induced acute kidney injury partly by regulating SIRT3/SOD2 pathway. *Front. Med.* **2023**, *9*, No. 1055252.
(56) Mayne, P. D. *Zilva's Clinical Chemistry in Diagnosis and Treatment*; ELBS: London, 1994.
(57) Hoivik, D. J.; Fisher, R. L.; Brendel, K.; Gandolfi, A. J.; Khairallah, E. A.; Cohen, S. D. Protein arylation precedes acetaminophen toxicity in a dynamic organ slice culture of mouse kidney. *Toxicol. Sci.* **1996**, *34* (1), 99−104.
(58) Mugford, C. A.; Tarloff, J. B. The contribution of oxidation and deacetylation to acetaminophen nephrotoxicity in female Sprague-Dawley rats. *Toxicol. Lett.* **1997**, *93* (1), 15−22.
(59) Rezende, T. P.; Corrêa, J. O. d. A.; Aarestrup, B. J.; Aarestrup, F. M.; De Sousa, O. V.; da Silva Filho, A. A. Protective effects of Baccharis dracunculifolia leaves extract against carbon tetrachloride- and acetaminophen-induced hepatotoxicity in experimental animals. *Molecules* **2014**, *19* (7), 9257−9272.
(60) Elmhdwi, M. F.; Muftah, S. M.; Elslimani, F. A.-z. Hepatoprotective effect of Ecballium Elaterium fruit juice against paracetamol induced hepatotoxicity in male albino rats. *Int. Curr. Pharm. J.* **2014**, *3*, 270−274, DOI: 10.3329/icpj.v3i5.18535.
(61) Mohamed, N. A.; Hassan, M. H.; Saleem, T. H.; Mohamed, S. A.; El-Zeftawy, M.; Ahmed, E. A.; Mostafa, N. A.; Hetta, H. F.; Hasan, A. S.; Abdallah, A. A. M. KIM-1 and GADDI-153 gene expression in paracetamol-induced acute kidney injury: effects of N-acetylcysteine, N-acetylmethionine, and N-acetylglucosamine. *Turk. J. Biochem.* **2022**, *47* (4), 409−416.
(62) Kandemir, F. M.; Kucukler, S.; Eldutar, E.; Caglayan, C.; Gülçin, İ. Chrysin protects rat kidney from paracetamol-induced oxidative stress, inflammation, apoptosis, and autophagy: a multi-biomarker approach. *Sci. Pharm.* **2017**, *85* (1), 4.
(63) Shen, H.; Sheng, L.; Chen, Z.; Jiang, L.; Su, H.; Yin, L.; Omary, B. M.; Rui, L. Mouse hepatocyte overexpression of NF-κB-inducing kinase (NIK) triggers fatal macrophage-dependent liver injury and fibrosis. *Hepatology* **2014**, *60* (6), 2065−2076.
(64) Aksun, S.; Gökcimen, A.; Kahyaoglu, F.; Demirci, B. The effect of Paracetamol exposure on hepatic and renal tissues during statin usage. *Turk. J. Biochem.* **2019**, *44* (1), 113−120.
(65) Hua, H.; Ge, X.; Wu, M.; Zhu, C.; Chen, L.; Yang, G.; Zhang, Y.; Huang, S.; Zhang, A.; Jia, Z. Rotenone protects against acetaminophen-induced kidney injury by attenuating oxidative stress and inflammation. *Kidney Blood Press. Res.* **2018**, *43* (4), 1297−1309.
(66) Ghonaim, A. H.; Hopo, M. G.; Ismail, A. K.; AboElnaga, T. R.; Elgawish, R. A.; Abdou, R. H.; Elhady, K. A. Hepatoprotective and renoprotective effects of silymarin against salinomycin-induced toxicity in adult rabbits. *Vet. World* **2022**, *15* (9), 2244.
(67) Onaolapo, O. J.; Adekola, M. A.; Azeez, T. O.; Salami, K.; Onaolapo, A. Y. l-Methionine and silymarin: A comparison of prophylactic protective capabilities in acetaminophen-induced injuries of the liver, kidney and cerebral cortex. *Biomed. Pharmacother.* **2017**, *85*, 323−333.
(68) Rafieian-Kopaie, M.; Nasri, H. Silymarin and diabetic nephropathy. *J. Renal Inj. Prev.* **2012**, *1* (1), 3−5.
(69) Wadhwa, K.; Pahwa, R.; Kumar, M.; Kumar, S.; Sharma, P. C.; Singh, G.; Verma, R.; Mittal, V.; Singh, I.; Kaushik, D.; Jeandet, P. Mechanistic insights into the pharmacological significance of silymarin. *Molecules* **2022**, *27* (16), 5327.
(70) Alomair, M. K.; Alobaid, A. A.; Almajed, M. A. A.; Alabduladheem, L. S.; Alkhalifah, E. A.; Mohamed, M. E.; Younis, N. S. Grape Seed Extract and Urolithiasis: Protection Against Oxidative Stress and Inflammation. *Pharmacogn. Mag.* **2023**, *19* (1), 117−127.
(71) Guendez, R.; Kallithraka, S.; Makris, D. P.; Kefalas, P. Determination of low molecular weight polyphenolic constituents in grape (*Vitis vinifera* sp.) seed extracts: Correlation with antiradical activity. *Food Chem.* **2005**, *89* (1), 1−9.
(72) Hassan, H. A.; Isa, A. M.; El-Kholy, W. M.; Nour, S. E. Testicular disorders induced by plant growth regulators: cellular protection with proanthocyanidins grape seeds extract. *Cytotechnology* **2013**, *65*, 851−862.
(73) Chen, Y.; Wen, J.; Deng, Z.; Pan, X.; Xie, X.; Peng, C. Effective utilization of food wastes: Bioactivity of grape seed extraction and its application in food industry. *J. Funct. Foods* **2020**, *73*, No. 104113.
(74) Ibrahim, A. K.; AL-Azawi, A. H. Nephro-protective effect of (Arachis hypogaea L.) peanut skin extracts on CCl4 induced kidney damage in mice. *Exp. Anim.* **2019**, *900* (1), No. 15.
(75) Kyei, S. K.; Eke, W. I.; Abdul-Karim, H.; Darko, G.; Akaranta, O. Phytochemicals from Peanut (Arachis hypogaea L.) skin extract with potential for pharmacological activity. *Curr. Bioact. Compd.* **2021**, *17* (9), 38−56.

https://doi.org/10.1021/acsomega.4c05534
ACS Omega 2024, 9, 35154−35169